Fiber Bragg Grating Sensor Based Mode Filtering Using Cosine Distance Metric

ROHAN SOMAN, KALEEESWARAN BALASUBRAMANIAM and PAWEL MALINOWSKI

ABSTRACT

Fiber Bragg grating (FBG) sensors are considered ideal for structural health monitoring (SHM) due to their small weight and size, ability to be embedded and ability to be multiplexed. So, FBG sensors are commonly used as strain sensors for SHM but their use for ultrasonic guided wave (GW) measurements is not common due to the low sensitivity. In the recent times, a renewed interest is seen in the use of FBG sensors for GW measurements using the edge reflection approach which increases the sensitivity several folds.

It has been reported, that the mechanism of the measurement of the incident GW is different based on the relative ratio of the wavelength of the incident GW (λ_{GW}) and the grating length (L) of the FBG sensor. For ratios $\lambda_{GW} / L \gg 1$ the propagating wave leads to uniform strain over the FBG resulting in the shift of the Bragg wavelength. For the $\lambda_{GW}/L \approx 1$ the FBG experiences non-uniform strain over the FBG which results in the distortion of the spectrum (widening or narrowing) of the peak. By separating these effects on the FBG, mode filtering may be achieved. In the previous work the mode filtering was achieved by scanning the entire reflectivity spectrum of the FBG (over 300 points). This approach is time consuming and hence has limited applicability for in-service SHM. Hence, a novel method which uses only measurements at 2 locations on the spectrum is proposed in this paper. The cosine distance in the waveforms is calculated and then used for identifying the mode. This information is then used for damage localization on a simple plate.

INTRODUCTION

Structural health monitoring (SHM) systems allow reduction in operation and maintenance cost and increase the reliability of the structure. As a result SHM systems are deployed on important infrastructure such as bridges, airplanes, oil platforms etc. The commonly used SHM techniques include vibration based SHM, strain based SHM, guided waves (GW) based SHM and electromechanical impedance based SHM techniques [1–4]. Each of these techniques have their own sets of advantages and disadvantages. For large 1-D and 2-D structures, GW based techniques are considered ideal. The

Rohan Soman*, Kaleeswaran Balasubramaniam, Pawel Malinowski. Institute of Fluid Flow Machinery, Polish Academy of Sciences, Gdansk, Poland. email: rsoman@imp.gda.pl

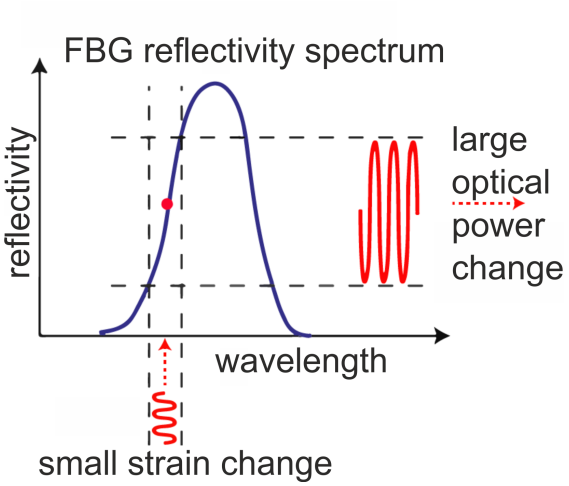

Figure 1. Edge filtering approach for increased sensitivity based on [10]

GW based techniques allow monitoring of large areas with relatively few sensors. Also, due to the small wavelengths of the the GW they are capable of detecting and localizing small damages which are highly desirable in aerospace structures. For the sensing of GW several different sensor systems such as piezoelectric sensors (PZT), macro fiber composites, optical fiber sensors etc. have been used. For non contact sensing acoustic transducers and laser Doppler vibrometer have also been used. The PZT based sensors are the standard, but the use of FBG sensors for GW sensing is on an increase.

The FBG sensors offer several advantages such as small size, ability to be multiplexed, ability to be embedded as well as the insensitivity to electrical and magnetic fields and as such are seen as ideal sensors. In the traditional approach uses the FBG sensors with a broadband laser source and the change in the reflected wavelength is tracked. The change in the reflected wavelength is proportional to the strain in the structure and may be used for transduction. This approach is ideal for static and quasi static measurements. For GW sensing where high sampling rates are necessary this approach is not ideal. Hence, the FBG sensors are employed in so-called edge filtering configuration (figure 1). In the edge filtering approach, a narrow band tunable laser is tuned on the reflectivity slope of the FBG. The reflectivity curve has a high slope and is linear in the middle section. As a result small shift in the position of the reflectivity leads to a large change in the optical power which is detected by the photodetector. This configuration amplifies the sensitivity of the sensor but also allows high speed sampling of the response. The edge filtering approach has been successfully used for SHM by several researchers [5–8]. The directionality was incorporated in the SHM algorithm by Soman et al [9]. An excellent review about the physics of the wave coupling and their use for SHM has been conducted by Soman et al. [10] and Wu et al. [11].

The major challenge in the use of GW for damage detection is their multimodal and dispersive nature. Several different modes (symmetric and antisymmetric fundamental and higher modes) propagate in the structure at the same time. These modes interact with structural features and damage and undergo mode conversion which increases the complexity of the signal processing. In most cases the excitation frequency is limited to the region where only the fundamental modes exist (A0 and S0). This simplifies the pro-

cessing to a certain degree but in case of complex components even the presence of two modes and their interactions makes it challenging. Hence, a methodology for mode separation or filtering are highly sought after. The work in this area can primarily be classified into excitation approaches and sensing approaches. The excitation approaches work towards selective excitation of one mode through the use special transducers (EMAT etc.), special attachments (use of wedges), or special arrangements [12–14]. These excitation systems are specialized and hence costly, or work for only a selected frequency range hence are not ideal. On the sensing side, most of the work is based on frequency-wave number techniques [15, 16]. These methods make use of multiple sensing locations and use the difference in the wavelength of the different modes to filter the waves. The multipoint measurement needed increases the number of sensors used and hence has limited applicability. Soman et al. have successfully used single FBG sensors for separating the S0 and A0 mode in a limited frequency range. They used the different mechanism of the coupling of the wave to the FBG based on the relative ratio of the FBG gauge length and the GW wavelength. This phenomena has also been reported by Coppola et al., Minardo et al., and Goossens et al. [17–19].

In the work by Soman et al. [20], the mechanisms were separated by recreating the reflectivity spectrum of the FBG for each time instance and then determining the mechanism. This approach although effective, needs 500 measurements for each actuator-sensor pair. This approach is too time consuming and hence too cannot be applied directly for SHM. In this paper the measurements from just 2 points on the spectrum of the FBG are used and the mode is determined based on the cosine distance. The approach allows identification of the propagating mode.

MODE FILTERING

In the work by Soman et al., the mechanisms were separated by recreating the reflectivity spectrum of the FBG for each time instance and then determining the mechanism. This approach although effective, needs 500 measurements for each actuator-sensor pair. This approach is too time consuming and hence cannot be applied directly for SHM. In this paper the measurements from just 2 points on the spectrum of the FBG are used and the mode is determined based on the cosine distance. The approach allows identification of the propagating mode. The concept is explained in detail in figure 2. As can be seen in the case of uniform strain, the change on either side of the slope is 180 $^{\circ}$ out of phase, while for non uniform strain, it will be in phase. Although this difference is trivial, the total effect of the propagating wave on the spectrum is a combination of the two mechanisms and need to be separated carefully.

In this, work the cosine distance metric is employed. The metric gives values between 0 and 2 with 0 showing similarity, 1 indicating orthogonality and 2 showing out of phase. The cosine distance is adopted as the values are irrespective of the relative amplitudes of the signal. Although care is taken to tune the laser at the point of maximum slope on either side, it might not be possible due to the distortion of the spectrum during deployment of the sensor. The cosine distance is computed by using the 'pdist' command in Matlab and the equation is given by equation.

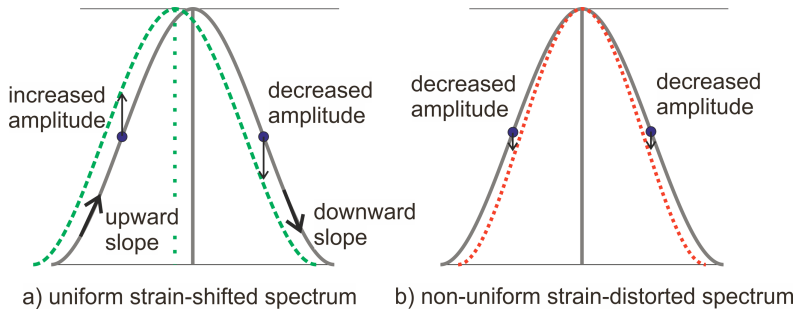

Figure 2. Effect of the different propagating GW wavelengths on FBG spectrum. Grey line shows spectrum in unstrained condition, a) green line shows shifted spectrum due to uniform strain b) red line shows distorted spectrum due to non-uniform strain. The purple dot shows the lased wavelengths on either side of the spectrum.

$$d_{cosine} = 1 - \frac{x_l x_r'}{\sqrt{(x_l x_l')(x_r x_r')}} \tag{1}$$

where x_l and x_r are measurements from the left and right side of FBG spectrum

Ofcourse the cosine distance is calculated to measure the similarity between two vectors. So the signals from the upward and downward slope of the FBG spectrum are acquired. For each time step, the vectors from the acquired time signal are determined by a moving Hann window centered at that time. The Hann window was chosen to minimize the leakage, while width of the window was determined iteratively based on the length of the excitation signal.

EXPERIMENTAL SETUP

The experimental is shown in figure 3. The FBG spectrum was scanned in the DC configuration to acquire the FBG spectrum and locations on the upward and downward slope were identified. The tunable laser was then tuned on these wavelengths successively and the GW measurements were recorded. The tunable laser, oscilloscope and the waveform generator are all synchronized and controlled through the Matlab instrument control toolbox.

The FBG sensor was polyimide coated fiber was with grating length 10 mm and was glued on the structure with NBA 107 adhesive. Other details on the equipment and setup may be found in [20].

RESULTS AND DISCUSSIONS

The figure 4 shows the measurement for the upward and downward slope (multiplied by -1) of the FBG spectrum. Visually, it seems that the signals are in phase with minor changes. The cosine distance between the two time signals for each time step is also plotted. The peaks in the measured time signal are identified using the 'findpeaks' command in Matlab. Given reasonable parameters for the separation of the peaks in time and minimum height, 7 peaks are identified. An envelope is used to smooth the

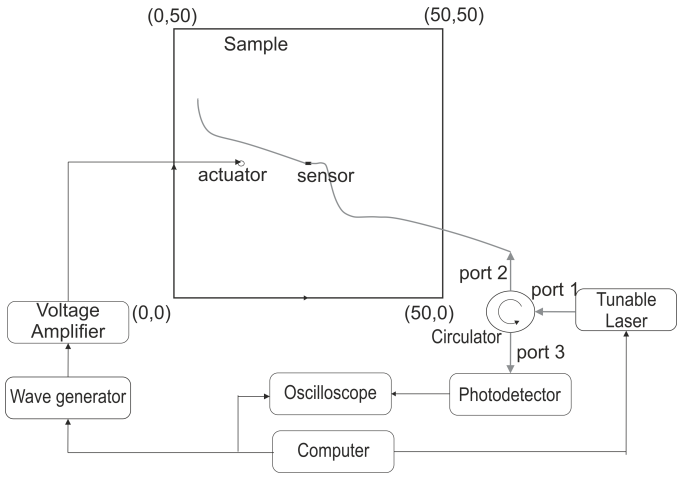

Figure 3. Schematic of the experimental setup

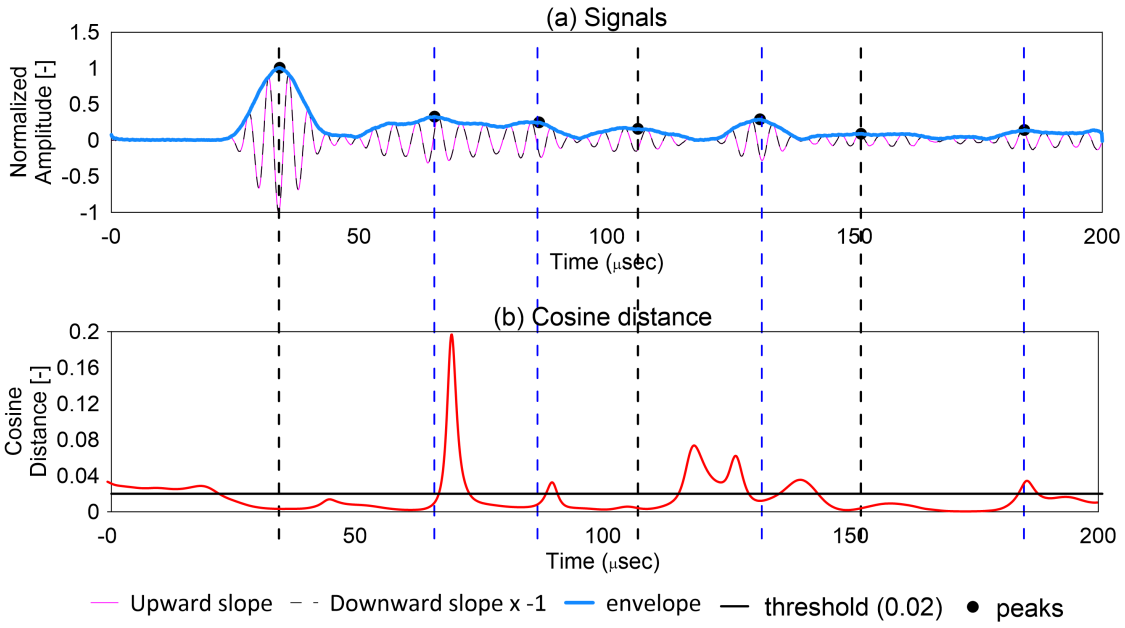

Figure 4. Acquired signal and cosine distance for 250 kHz

signal and ensure reliable peak detection. The cosine distance at each of the 7 points is then determined from the cosine distance plot. If the cosine distance exceeds 0.02 (chosen as threshold) within 10μs of the identified peak, the peak corresponds to the A0 wave packet. If the value does not exceed the 0.02, then the wave arrival corresponds to S0. The 10μs is chosen based on the half width of the excitation signal. The peaks are color-coded in figure 4 with black dotted lines indicating S0 arrival and blue dotted lines indicating A0 arrivals.

In order to verify if indeed the identified modes are correct. The wave arrivals were compared with the modes separated by the method outlined in the previous work using the entire swept spectrum. They are shown in figure 5.

Similar study was also tried for 50 kHz. It can be clearly seen, that the cosine distance does not exceed 0.02 for any of the peaks. This is because, the relative ratio of

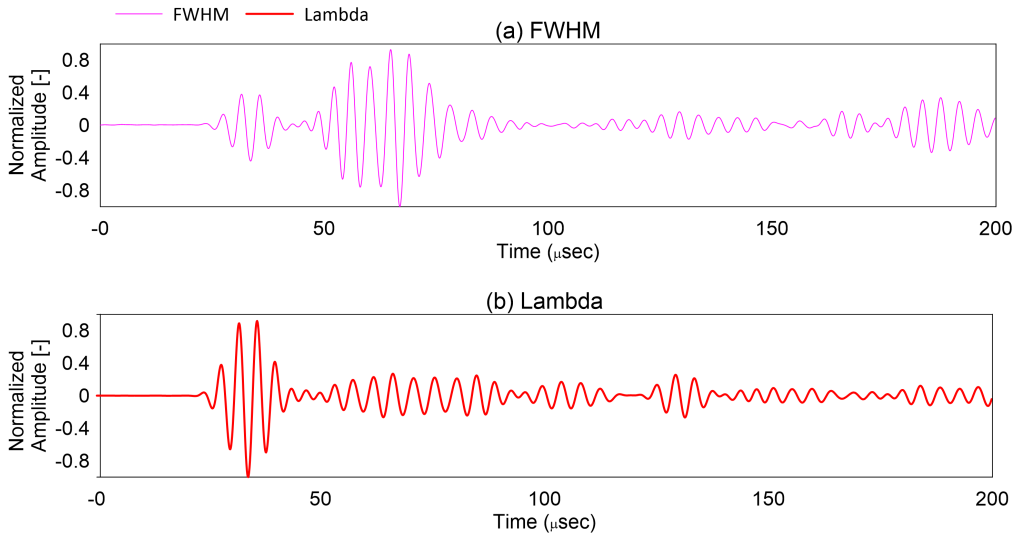

Figure 5. Mode separated signal based on change in FWHM and change in λ at 250 kHz

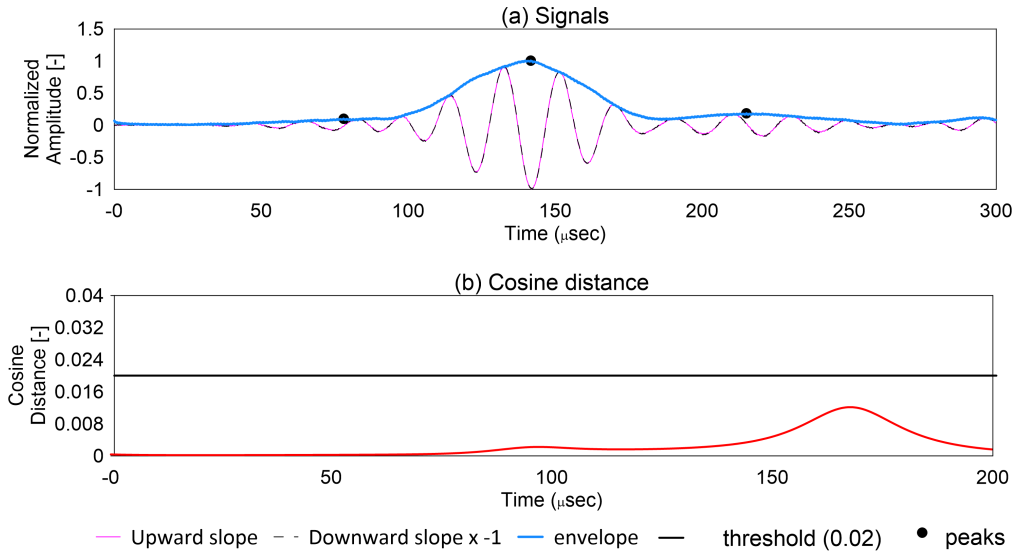

Figure 6. Acquired signal and cosine distance for 50 kHz

wavelength to gauge length for both the A0 and S0 modes for 50 kHz is significantly $\gg$ 1 and results in only shift in the spectrum. Hence the signals are in phase throughout.

The difference in the cosine distance is only significant at 200 kHz and 250 kHz, as only at that frequency the wavelength ratio to the FBG gauge length are in different domains as shown by Table I.

CONCLUSIONS AND FUTURE WORK

Based on the results shown it can be seen that for wavelengths where the relative ratio of the GW wavelength to the gauge length are in different domains, the mechanism for the coupling of the wave in the FBG sensor is different. This can indeed be leveraged to

TABLE I. WAVELENGTHS FOR THE WAVELENGTHS FOR THE A0 AND S0 MODES IN 1 MM THICK ALUMINUM PLATE

Frequency [kHz]	λ_{GW}/L ratio (Wavelength in mm) for A0	λ_{GW}/L ratio (Wavelength in) for S0
50	1.35 (13.5)	10.17 (101.7)
100	0.96 (9.6)	4.72 (47.2)
150	0.78 (7.8)	3.48 (34.8)
200	0.65 (6.5)	2.59 (25.9)
250	0.56 (5.6)	2.00 (20.0)

perform mode filtering using measurements at the same point. In this work, the limitation of needing a large number of measurements to acquire the mechanism is addressed. It is shown that measurements at only two points on the FBG spectrum are sufficient to identify the mode.

The cosine distance which is an efficient metric for comparison of the two signals which is independent of the relative magnitudes is used for determining the difference in the two measurements. The cosine distance value corresponding to the peak if it exceeds a certain threshold then the peak corresponds to the A0 mode arrival. If it does not exceed, the threshold the mode is a S0 mode. It is conceded that the threshold has to be determined empirically and method to formally determine it needs to be in place. Besides the metric is sensitive to the amount of noise to the data and the preprocessing carried out. These parameters too need to be determined which is identified as the future work. Once these parameters are established, the mode filtering may be used to enhance damage detection techniques.

ACKNOWLEDGMENT

The research was supported by the project "Study of fibre optic sensor arrays for structural health monitoring based on guided waves" (2019/33/B/ST8/01699) granted by National Science Center, Poland. The authors are also grateful to TASK-CI for allowing the use of their computational resources. The opinions expressed in this paper do not necessarily reflect those of the sponsors.

REFERENCES

1. Sha, G., R. Soman, M. Radzieński, M. Cao, W. Ostachowicz, and H. Zuo. 2021. "A two-step method for additional mass identification in beam structures by measurements of natural frequencies and guided waves," *Measurement*, 186:110049.
2. Kakei, A., J. Epaarachchi, M. Islam, and J. Leng. 2018. "Evaluation of delamination crack tip in woven fibre glass reinforced polymer composite using FBG sensor spectra and thermo-elastic response," *Measurement*, 122:178–185.
3. Mitra, M. and S. Gopalakrishnan. 2016. "Guided wave based structural health monitoring: A review," *Smart Materials and Structures*, 25(5):053001.

4. de Castro, B. A., F. G. Baptista, and F. Ciampa. 2019. "New signal processing approach for structural health monitoring in noisy environments based on impedance measurements," *Measurement*, 137:155–167.
5. Yu, F., O. Saito, and Y. Okabe. 2021. "Laser ultrasonic visualization technique using a fiber-optic Bragg grating ultrasonic sensor with an improved adhesion configuration," *Structural Health Monitoring*, 20(1):303–320.
6. Xu, W., Q. Wu, H. Zhang, C. Gong, R. Wang, J. Lu, and K. Xiong. 2021. "Debonding monitoring of CFRP T-joint using optical acoustic emission sensor," *Composite Structures*, 273:114266.
7. Navratil, A., J. Wee, and K. Peters. 2021. "Ultrasonic frequency response of fiber Bragg grating under direct and remote adhesive bonding configurations," *Measurement Science and Technology*, 33(1):015204.
8. Lambinet, F. and Z. Sharif Khodaei. 2021. "Development of Hybrid Piezoelectric-Fibre Optic Composite Patch Repair Solutions," *Sensors*, 21(15):5131.
9. Soman, R., K. Balasubramaniam, A. Golestani, M. Karpiński, and P. Malinowski. 2020. "A two-step guided waves based damage localization technique using optical fiber sensors," *Sensors*, 20(20):5804.
10. Soman, R., J. Wee, and K. Peters. 2021. "Optical Fiber Sensors for Ultrasonic Structural Health Monitoring: A Review," *Sensors*, 21(21):7345.
11. Wu, Q., Y. Okabe, and F. Yu. 2018. "Ultrasonic structural health monitoring using fiber Bragg grating," *Sensors*, 18(10):3395.
12. Giurgiutiu, V. 2005. "Tuned Lamb wave excitation and detection with piezoelectric wafer active sensors for structural health monitoring," *Journal of Intelligent Material Systems and Structures*, 16(4):291–305.
13. Stepinski, T., M. Mańka, and A. Martowicz. 2017. "Interdigital Lamb wave transducers for applications in structural health monitoring," *NDT & E International*, 86:199–210.
14. Moghadam, P. Y., N. Quaegebeur, and P. Masson. 2016. "Design and optimization of a multi-element piezoelectric transducer for mode-selective generation of guided waves," *Smart Materials and Structures*, 25(7):075037.
15. Purcell, F. A., M. Eaton, M. Pearson, and R. Pullin. 2020. "Non-destructive evaluation of isotropic plate structures by means of mode filtering in the frequency-wavenumber domain," *Mechanical Systems and Signal Processing*, 142:106801.
16. Flynn, E. B., S. Y. Chong, G. J. Jarmer, and J.-R. Lee. 2013. "Structural imaging through local wavenumber estimation of guided waves," *Ndt & E International*, 59:1–10.
17. Coppola, G., A. Minardo, A. Cusano, G. Breglio, L. Zeni, A. Cutolo, A. M. Calabro, M. Giordano, and L. Nicolais II. 2001. "Analysis of feasibility on the use of fiber Bragg grating sensors as ultrasound detectors," in *Smart Structures and Materials 2001: Sensory Phenomena and Measurement Instrumentation for Smart Structures and Materials*, International Society for Optics and Photonics, vol. 4328, pp. 224–232.
18. Minardo, A., A. Cusano, R. Bernini, L. Zeni, and M. Giordano. 2004. "Fiber Bragg grating as ultrasonic wave sensors," in *Second European Workshop on Optical Fibre Sensors*, International Society for Optics and Photonics, vol. 5502, pp. 84–87.
19. Goossens, S., F. Berghmans, and T. Geernaert. 2020. "Spectral Verification of the Mechanisms behind FBG-Based Ultrasonic Guided Wave Detection," *Sensors*, 20(22):6571.
20. Soman, R., M. Radzienski, P. Kudela, and W. Ostachowicz. 2022. "Guided waves based damage localization based on mode filtering using fiber Bragg grating sensors," *Smart Materials and Structures*, 31(9):095025.